



# Transmission Electron Microscopic and X-ray Diffraction Based Study of Crystallographic Bibliography Demonstrated on Silver, Copper and Titanium Nanocrystals: State of the Art Statical Review

Md. Khalid Hossain Shishir <sup>a</sup>, Sumaiya Islam Sadia <sup>a</sup>,  
Shanawaz Ahmed <sup>a</sup>, Allah Rakha Aidid <sup>a</sup>,  
Md. Masud Rana <sup>a,b</sup>, Md. Mehedi Hasan <sup>c</sup>, Sazal Kumar <sup>a,d</sup>,  
Raton Kumar Bishwas <sup>e</sup> and Md. Ashraful Alam <sup>a,e\*</sup>

<sup>a</sup> Department of Applied Chemistry and Chemical Engineering (ACCE), Islamic University (IU), Kushtia-7003, Bangladesh.

<sup>b</sup> Hydrogen Energy Research Laboratory, Korea Institute of Energy Technology (KENTECH), 200 Hyeoksins-ro, Naju-Si, Jeonnam-58330, Republic of Korea.

<sup>c</sup> Bangladesh Reference Institute for Chemical Measurements (BRiCM), Dhaka-1205, Bangladesh.

<sup>d</sup> School of Environmental and Life Sciences, The University of Newcastle (UoN), Callaghan, NSW-2308, Australia.

<sup>e</sup> Institute of Glass and Ceramic Research and Testing (IGCRT), Bangladesh Council of Scientific and Industrial Research (BCSIR), Dhaka-1205, Bangladesh.

## Authors' contributions

This work was carried out in collaboration among all authors. All authors read and approved the final manuscript.

## Article Information

DOI: <https://doi.org/10.9734/ajacr/2024/v15i3287>

## Open Peer Review History:

This journal follows the Advanced Open Peer Review policy. Identity of the Reviewers, Editor(s) and additional Reviewers, peer review comments, different versions of the manuscript, comments of the editors, etc are available here: <https://www.sdiarticle5.com/review-history/116728>

**Review Article**

**Received: 06/03/2024**

**Accepted: 10/05/2024**

**Published: 14/05/2024**

\*Corresponding author: Email: [ashrafulalam@bcsir.gov.bd](mailto:ashrafulalam@bcsir.gov.bd);

**Cite as:** Shishir, M. K. H., Sadia, S. I., Ahmed, S., Aidid, A. R., Rana, M. M., Hasan, M. M., Kumar, S., Bishwas, R. K., & Alam, M. A. (2024). Transmission Electron Microscopic and X-ray Diffraction Based Study of Crystallographic Bibliography Demonstrated on Silver, Copper and Titanium Nanocrystals: State of the Art Statical Review. *Asian Journal of Applied Chemistry Research*, 15(3), 1–19. <https://doi.org/10.9734/ajacr/2024/v15i3287>

## ABSTRACT

This statistical review compares the crystallographic structures of functional nanocrystals composed of silver (Ag), copper (Cu) and titanium (Ti) using transmission electron microscopy (TEM) and X-ray diffraction (XRD) analyses. TEM provides high-resolution imaging to directly visualize individual nanoparticles' size, internal shape and crystallinity. Statistical analysis quantifies variations in lattice parameters, crystal structure, size distributions, phase compositions, lattice strains, preferred orientation and lattice volume of these three crystalline nanomaterials. The review highlights the complementary roles of TEM and XRD in comprehensive Ag, Cu and Ti nanocrystalline materials characterization. The crystallographic functional parameters of Ag were  $2\theta = 38.1^\circ$  (111),  $44.3^\circ$  (200) and  $64.4^\circ$  (220); for Cu crystal  $43.3^\circ$  (111),  $50.4^\circ$  (200),  $74.1^\circ$  (220),  $89.9^\circ$  (311) and  $95.1^\circ$  (222) and  $35.1^\circ$  (100),  $38.4^\circ$  (002),  $40.2^\circ$  (101),  $53.0^\circ$  (102),  $63.0^\circ$  (103),  $70.7^\circ$  (110),  $76.2^\circ$  (112),  $82.3^\circ$  (201) demonstrated for Ti nanocrystals. The crystallographic predominant plane or Miller indices were also revealed by selected area electron diffraction (SAED) on TEM. The FCC structure of Ag and Cu is shown in larger lattice volumes compared to the HCP structure of Ti and prefer oriented. The degree of crystallinity of Ti, Cu and Ag nanocrystalline materials was observed at 90.0%, 98.0% and 100.0% respectively. This quantitative comparison provides valuable insights into the structural property relationships in these nanocrystals, enabling rational design strategies for optimizing their performance in various functional applications.

*Keywords: Crystallographic bibliography; nanocrystals; phase; transmission electron microscopic; x-ray diffraction.*

## 1. INTRODUCTION

The accurate characterization and comparison of functional nanocrystals is essential to advancing many technological applications in nanotechnology [1]. Nanomaterials are very beneficial because of their great catalytic activity, decreased size and enhanced solubility [1]. The arrangements of atoms or molecules that are structured at the nanoscale are known as crystalline nanomaterials [2]. Their diminutive dimensions and expansive surface area, often exhibit unique properties that render them valuable across diverse sectors such as electronics, healthcare and energy storage [2]. The mechanical strength, wide surface area, superior electrical conductivity, customizable optical qualities, thermal stability and conductivity and customizable chemical reactivity are the benefits that crystalline nanostructures [2]. Nanomaterials can have extraordinary mechanical qualities including high strength and stiffness of their crystalline structure which is useful for structural functional applications [3-5]. Methods such as XRD which offer insights into crystal structure and lattice parameters are widely employed for the characterization of the crystalline properties of Ag nanoparticles [6,7]. Depending on variables including synthesis conditions and method, Ag nanoparticles can exhibit various crystalline configurations including face-centered cubic (FCC) or hexagonal close-packed (HCP) structures. [6,7]. Biomedical

technology, sensing and catalysis are impacted by these features which also affect their physical, chemical and optical behaviour [6,7]. The synthesis process and circumstances of Cu nanoparticles can influence their crystalline characteristics [8]. They usually have a crystalline structure depending on their size, shape and surface characteristics [8]. The arrangement can be either body-centered cubic (BCC) or face-centered cubic (FCC) in this structure [8]. Their chemical and physical characteristics, including mechanical strength, conductivity and catalytic activity are influenced by their crystallinity [8].

Certain characteristics of Ti nanoparticles like size, surface treatment and production method can lead to crystalline qualities [9]. Their optical behaviour, mechanical strength and chemical reactivity can all be impacted by these characteristics [9]. Ti nanoparticles can have a variety of crystalline forms including anatase, rutile or anatase-rutile mixed phases depending on the production method [9]. Their performance in a variety of applications including energy storage, biomedical devices and catalysis is impacted by these architectures [9]. Nanoparticles made of Ti, Cu and Ag each have special qualities and uses [10]. Due to their well-known antibacterial qualities, Ag nanoparticles are beneficial in consumer goods and medical equipment [10]. Copper nanoparticles are useful in electronics, and catalysis and they also show

antibacterial properties [11]. Ti nanoparticles are used in sunscreen, medical implants and aircraft because of their strength, lightweight and corrosion resistance [11]. Excellent optical qualities are characteristic of Ag nanoparticles [12]. Strong mechanical properties characterize Cu nanoparticles [12]. Ti nanoparticles are recognized for their high strength-to-weight ratio, corrosion resistance and compatibility with biological systems [12]. The reactivity of Ag nanoparticles is high [13]. Certain acids and oxidizing substances cause Cu nanoparticles to react [13]. In general, Ti nanoparticles are less reactive than those of Ag and Cu, although at high temperatures they can react with strong acids and bases [13]. Ag nanoparticles are widely employed in electronics, catalysts, antimicrobial coatings and wound dressings [14]. Cu nanoparticles find applications in catalysts, antimicrobial surfaces, printed electronics and conductive inks [14]. Ti nanoparticles find application in water purification systems, sunscreen formulations, medicinal implants and aeronautical materials [14].

Since Ag nanoparticles are widely used in consumer goods, there are worries over their possible harm to people and ecosystems [15]. Nanoparticles of Cu are vital trace elements for many species of copper [15]. Although long-term consequences are still being investigated, Ti nanoparticles are generally considered safer than Ag and Cu nanoparticles [15]. As Ag is more expensive than Cu and Ti, Ag nanoparticles are rather pricey [16]. Compared to Ag, Cu nanoparticles are more affordable and more widely available [16]. Because of their energy-intensive manufacturing method, Ti nanoparticles can be expensive; nevertheless, their availability depends on demand and manufacturing capacity [16]. We hope to clarify the similarities and contrasts among these materials' crystallographic properties through statistical analysis, providing insight into their functional uses and directing future research activities.

## 2. MATERIALS AND METHODS

Three essential ingredients are required to acquire nanoparticles, particularly Cu nanoparticles. Initially, a substance that releases ions. Furthermore, the acquisition of atoms needs the presence of a reducing agent to furnish electrons. Under optimal temperature and pH circumstances, the surfactant facilitates the aggregation of atoms the reducing agent

produces into nanoparticles. Diverse metallic nanoparticles can be synthesized using various physical, chemical and biological techniques [32]. Chemical methods provide precise control over the size, growth, shape and dispersion of particles by optimizing reaction parameters, including reaction duration, pH and choice of solvent. So, chemical methods like sol-gel, chemical reduction, microwave-assisted, hydrothermal etc are mentioned in this manuscript. Table 1, Nanoparticles have been synthesized via a variety of methods with different precursors. For Ti nanoparticles, precursors like titanium tetrachloride ( $TiCl_4$ ), Titanium isopropoxide (TTIP) and Tetrabutyl Titanate have been used.  $AgNO_3$  has been used as Ag nanoparticle precursors. In the case of Cu nanoparticles, precursors like  $CuSO_4$ ,  $Cu(NO_3)_2$ ,  $CuCl_2$  etc are used [17-31].

## 3. CHARACTERIZATION

XRD and TEM were employed in investigating crystallographic textures of nanocrystals and have been explored in this review as indicated in Table 2 [33-37].

## 4. RESULTS AND DISCUSSION

### 4.1 X-ray Diffraction (XRD) Analysis

XRD analysis is an effective method employed for examining the crystal structure of materials including Ag, Cu and Ti crystals [38]. When X-ray radiation strikes a crystalline substance, it interacts with the atoms within the crystal lattice planes, leading to constructive and destructive interference patterns [38]. These interference patterns are recorded as diffraction or reflection which can be analyzed to determine various structural properties of the material [39]. The locations and strengths of the diffraction pattern can be utilized to ascertain both the crystal system and the lattice parameters of the crystals [39]. The widening of the diffraction pattern can be attributed to the limited size of the crystallites and the existence of strain within the crystal lattice [39]. In a pure Ag crystal, the XRD pattern will exhibit distinct diffraction corresponding to the different crystallographic planes present in the crystal structure. The XRD pattern of a pure Ag crystal explored the characteristics of its face-centered cubic (FCC) crystal structure shown in Fig. 2 [40]. In the XRD pattern of pure Ag crystals, the most notable diffractions are typically observed at the following positions

Table 1. Various methods for Ag, Cu and Ti production

Methods	Precursors	Conditions	References
<b>Crystalline Silver Nanoparticles</b>			
Sol-Gel	TEOS (Tetraethyl orthosilicate), AgNO <sub>3</sub>	Solvent: Ethanol (exerting nitric acid promotes hydrolysis). Ratio: TEOS: Ethanol: H <sub>2</sub> O = 1:4:4.	[17]
Chemical reduction	AgNO <sub>3</sub>	Solvent: Water. Reducing agent: Ascorbic acid. Stabilizer: PVP. Temperature: 80.0 °C, 12.0 h.	[18]
Ultrasound irradiation	AgNO <sub>3</sub>	Solvent: Water. Reducing and stabilizing agent: fructose and starch.	[19]
Hydrothermal	AgNO <sub>3</sub>	Two ion exchange processes: i) Chabazite tuff with NH <sub>4</sub> <sup>+</sup> ii) Latter ions change with silver Temperature: 400.0 °C, 1.0 h.	[20]
<b>Crystalline Copper Nanoparticles</b>			
Wet chemical	CuSO <sub>4</sub>	Solvent: Water or Ethylene glycol. Reducing agent: Ascorbic acid. Stabilizer: PVP. Temperature: 80.0 °C.	[21]
Wet chemical	CuCl <sub>2</sub>	Solvent: Ethanol. Reducing agent: NaBH <sub>4</sub> . Stabilizer: PVP. Sealed for 8.0 h.	[22]
Wet chemical	Cu (NO <sub>3</sub> ) <sub>2</sub>	Solvent: Water + Ethylene glycol. Reducing agent: NaBH <sub>4</sub> . Stabilizer: Tergitol NP-9. Temperature: Room temperature, 2.0 h.	[23]
Microwave-assisted	CuSO <sub>4</sub> .5H <sub>2</sub> O	Solvent: Ethylene glycol. Reducing agent: NaH <sub>2</sub> PO <sub>2</sub> .H <sub>2</sub> O. Stabilizer: PVP.	[24]
Sonochemical	CuSO <sub>4</sub>	Solvent: Water. Reducing agent: Na <sub>2</sub> H <sub>4</sub> . Stabilizer: PVP.	[25]
Microwave	CuCl <sub>2</sub>	Solvent: Water + Ethylene glycol.	[26]

Methods	Precursors	Conditions	References
		Reducing agent: Ethylene glycol + H <sub>2</sub> . Stabilizer: Sodium laurate.	
<b>Crystalline Titanium nanoparticles</b>			
Sol-Gel	Ti (OH) <sub>4</sub>	Solvent: Basic medium. Triethanolamine increases the nucleation rate. Temperature: 100.0 °C, 24.0 h and 140.0 °C, 72.0 h.	[27]
Co-precipitation	TTIP	Solvent: Mixture of methanol and ethanol. Calcinated below 500.0 °C.	[28]
Hydrothermal	Pure TiO <sub>2</sub>	Temperature: Room temperature. Solvent: NaOH and KOH. Calcinated at 250.0 °C, 2.0 h.	[29]
Solvothermal	Tetrabutyl Titanate	Temperature: 200.0 °C, 48.0 h. Both oleic acid and dodecyl amine performed as capping surfactants.	[30]
Wet chemical	TiCl <sub>4</sub>	Temperature: 300.0 °C, 10.0 h. Solvent: HCl Polyethylene glycol (PEG-1000) was used. Temperature: 80.0 °C, 2.0 h.	[31]

**Table 2. Crystallographic bibliographic parameters of Ag, Cu and Ti nanocrystals**

SI No.	Crystallographic bibliography parameters		Reference
01.	XRD	Lattice parameters, axial parameters, angular parameters, strain, lattice volume, microstrain, crystal structure, crystal shape, preferred orientation, crystallinity, crystal size, interplanar distance and crystal plane or miller indices.	[33-34]
02.	TEM	Internal morphology, strain, defect, orientation, shape, structure, volume fraction, axial parameters, angular parameters, selected area diffraction plane or Miller indices, nanobeam diffraction onto the plane, the stress of crystal, preferred orientation, grain boundary, particle sizes and dislocation density of the nanocrystals.	[34-37]

(expressed in terms of the Miller indices (h k l) and the corresponding interplanar spacing (d) values): (111) plane:  $d = 2.359 \text{ \AA}$ , (200) plane:  $d = 2.044 \text{ \AA}$ , (220) plane:  $d = 1.445 \text{ \AA}$ , (311) plane:  $d = 1.231 \text{ \AA}$ , (222) plane:  $d = 1.179 \text{ \AA}$  [41,42]. The relative intensities of these diffractions follow a pattern that is determined by the structure factor and the multiplicity of the planes [43]. In the case of an FCC crystal like Ag, the most intense diffraction typically corresponds to the (111) plane, followed by the (200), (220), (311) and (222) planes in decreasing order of intensity in Fig. 1. The prominent diffraction in the XRD pattern of pure Ag is (111) plane:  $2\theta \approx 38.1^\circ$ , (200) plane:  $2\theta \approx 44.3^\circ$ , (220) plane:  $2\theta \approx 64.4^\circ$  [43-45].

The XRD pattern obtained from a pure Cu crystal is characterized by distinct reflection corresponding to the different crystallographic planes present in the face-centered cubic (FCC) structure of copper in Fig. 2 [46]. The primary diffraction in the XRD pattern of a pure Cu crystal is commonly detected at the following angles at  $2\theta$  values and corresponding crystallographic planes as  $43.3^\circ$  (111) plane,  $50.4^\circ$  (200) plane,  $74.1^\circ$  (220) plane,  $89.9^\circ$  (311) plane and  $95.1^\circ$  (222) plane [46,47,49]. The relative intensities of these diffractions follow the pattern (111) > (200) > (220) > (311) > (222) in Fig. 1 [48]. The XRD

pattern of pure Cu crystal also exhibits additional diffraction at higher angles, corresponding to other crystallographic planes but with lower intensities [48]. The XRD profile of a pure Ti crystal depends on its crystal structure and lattice parameters [50]. At room temperature, Ti possesses a hexagonal close-packed (HCP) crystal structure, commonly referred to as the alpha ( $\alpha$ ) phase and its XRD pattern will exhibit characteristic diffraction corresponding to the allowed diffraction planes in the HCP structure in Fig. 2 (c) [50]. The prominent diffraction in the XRD pattern of pure Ti crystal is typically observed at the following  $2\theta$  (Bragg) angles as (100) plane:  $2\theta \approx 35.1^\circ$ , (002) plane:  $2\theta \approx 38.4^\circ$ , (101) plane:  $2\theta \approx 40.2^\circ$ , (102) plane:  $2\theta \approx 53.0^\circ$ , (103) plane:  $2\theta \approx 63.0^\circ$ , (110) plane:  $2\theta \approx 70.7^\circ$ , (112) plane:  $2\theta \approx 76.2^\circ$ , (201) plane:  $2\theta \approx 82.3^\circ$  [51-53]. The relative intensities of these diffractions, as well as the presence of additional diffraction at higher angles, can provide information about the preferred orientation in texture and crystallographic purity of the Ti crystal [55]. Additionally, the Ti sample may experience a phase transformed to the beta ( $\beta$ ) phase, also known as the body-centered cubic (BCC) structure, if it is exposed to high temperatures or specific heat treatments [54]. In these situations, distinct diffraction that corresponds to the  $\beta$ -Ti phase would be visible in the XRD pattern [54].

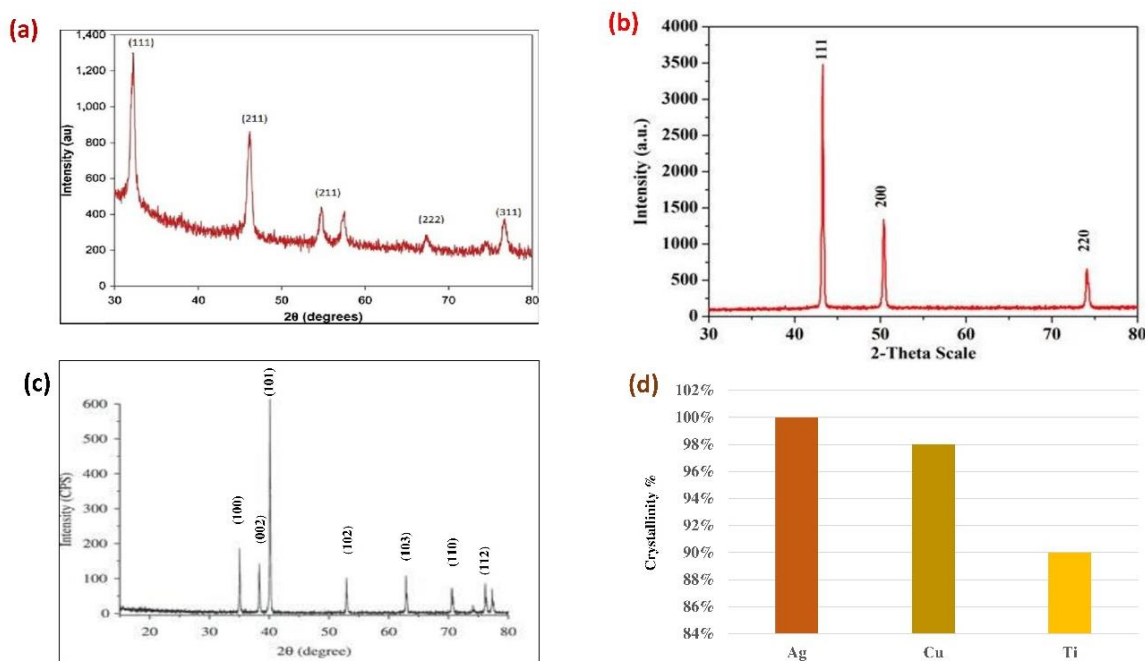


**Fig. 1. (a) XRD profile of pure Ag [56], (b) Cu [57], (c) Ti crystals [58] and (d) relative crystallinity of Ag, Cu and Ti [59-61] nanocrystals**

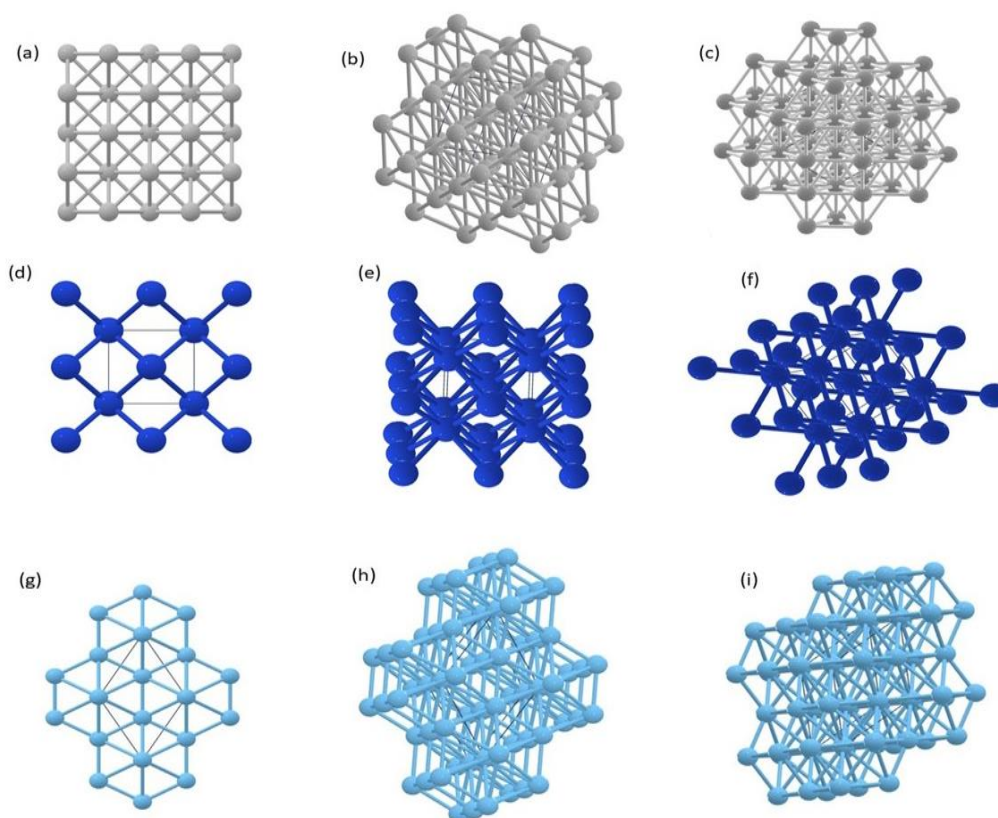


**Fig. 2. (a), (b), (c) crystal structure of Ag is face-centered cubic (FCC); (d), (e), (f) Cu crystal structure is face-centered cubic (FCC).; (g), (h), (i) crystal structure of Ti is hexagonal close-packed (HCP) [63]**

The percentage of crystallinity or the degree of crystallinity refers to the fraction of a material that is crystalline (has a highly ordered atomic structure) as opposed to amorphous (lacks long-range atomic order) [95]. The degree of crystallinity can vary depending on the material and the processing conditions [95]. Pure Ag is a highly crystalline metal with a typical degree of crystallinity close to 100.0 % [59]. Pure Cu is also highly crystalline with a typical degree of crystallinity around 98.0 % [60]. Pure Ti is a crystalline metal but its degree of crystallinity can vary depending on the processing conditions. Typically, the degree of crystallinity for pure Ti is around 90.0 % [61]. For highly pure and well-processed metals, the percentage of crystallinity can approach 100.0 % [102]. However, in practical applications, it's rare to achieve complete crystallinity due to factors like impurities, defects and processing conditions [62].

The preferred orientation also known as texture or crystallographic texture of a material refers to the preferential alignment of crystallites (grains)

in a particular direction relative to the sample's geometry or processing conditions [96]. The preferred orientation can significantly influence the material's properties such as mechanical strength, electrical conductivity and corrosion resistance [64]. Here's a comparative overview of the preferred orientation of Ag, Cu and Ti crystals. Ag crystals typically exhibit a strong preferred orientation in the (111) direction when deposited as thin films or coatings [65]. This favoured alignment is due to the reduced surface energy of the (111) plane within the face-centered cubic (FCC) arrangement of Ag [65]. The (111) texture can enhance the electrical conductivity and overall performance of Ag in electronic and optoelectronic applications. Like Ag, Cu also has an FCC crystal structure and it tends to develop a preferred orientation along the (111) direction when deposited as thin films or coatings [66]. On the other hand, Ti possesses a hexagonally close-packed crystal structure (HCP) and its preferred orientation can vary depending on the processing conditions and the specific application. In many cases, Ti exhibits a strong (0002) basal plane texture which is

beneficial for enhancing mechanical properties like strength and fatigue resistance [67]. Overall while Ag and Cu tend to exhibit a strong (111) texture due to their FCC structure, titanium's preferred orientation is more dependent on the specific processing conditions and application requirements with the (0002) basal plane texture being commonly observed [97].

#### 4.1.1 Lattice Strain and Lattice Volume Analysis

The lattice strain in a crystal structure is a measure of the deformation or distortion of the crystal lattice from its ideal, unstrained configuration [98]. The lattice strain can arise due to various factors such as the presence of impurities, defects or external forces applied to the crystal [68]. To compare the lattice strain values of Ag, Cu and Ti crystals, their crystal structures and the factors that contribute to lattice strain in each are considered. The lattice parameter ( $a$ ) for Ag: 4.0862 Å (at 25.0 °C) is found crystal shape [69]. The lattice strain of Ag was determined to be 0.00219 % in previous research [105]. The lattice strain in silver can occur due to factors such as impurities or dislocations. However, it's generally low due to the close-packed arrangement of atoms in its FCC structure [99]. Generally, Ag has a relatively low lattice strain due to its high ductility and ability to accommodate deformations. On the other hand, the lattice parameter ( $a$ ) for Cu: 3.6150 Å (at 25.0°C) is also found in the structure [71]. The lattice strain of Cu was determined to be 1.39 % in previous research [103]. Cu is also a ductile metal but it may exhibit slightly higher lattice strain compared to silver

due to its higher stacking fault energy and higher propensity for forming dislocations [104]. Again, lattice parameters ( $a$  and  $c$ ) for Ti: 2.9506 Å and 4.6855 Å (at 25.0 °C) respectively for HCP Ti crystal were investigated [71]. In the hexagonally close-packed (HCP) crystal structure of Ti, the conventional lattice strain is often described using the  $c/a$  ratio which is the ratio of the lattice parameters  $c$  is the height of the unit cell and an edge length of the basal plane. The standard or commonly accepted  $c/a$  ratio for titanium is ( $c/a$ ) Ti  $\approx$  1.587 % [101]. Ti generally exhibits higher lattice strain compared to Ag and Cu due to its crystal structure and lower ductility in Fig. 3 [100]. In the hexagonal close-packed (HCP) phase which remains stable at room temperature, the lattice strain may be notable owing to the hexagonal packing configuration. However, at elevated temperatures, Ti can adopt a BCC structure with lower lattice strain [54].

The lattice volume of a crystal denotes the volume occupied by the unit cell within its crystal lattice arrangement. It is determined by the size of the unit cell and the arrangement of atoms within it [72]. To compare the lattice volumes of Ag, Cu and Ti crystals, identify their crystal structures and lattice parameters. The lattice volume correlates directly with both the crystal structure and the lengths of the unit cell edges. For Ag, lattice volume ( $V$ ) =  $a^3 = (4.0862 \text{ \AA})^3 = 68.30 \text{ \AA}^3$  [73]; for Cu, lattice volume ( $V$ ) =  $a^3 = (3.6150 \text{ \AA})^3 = 47.23 \text{ \AA}^3$  [74] and for Ti, lattice volume ( $V$ ) =  $(0.866 \times a^2 \times c) = (0.866 \times (2.9506 \text{ \AA})^2 \times 4.6855 \text{ \AA}) = 35.10 \text{ \AA}^3$  [75]. Based on the calculations, the order of the lattice volumes from largest to smallest is Ag (FCC) > Cu (FCC) > Ti (HCP) in Fig. 4.

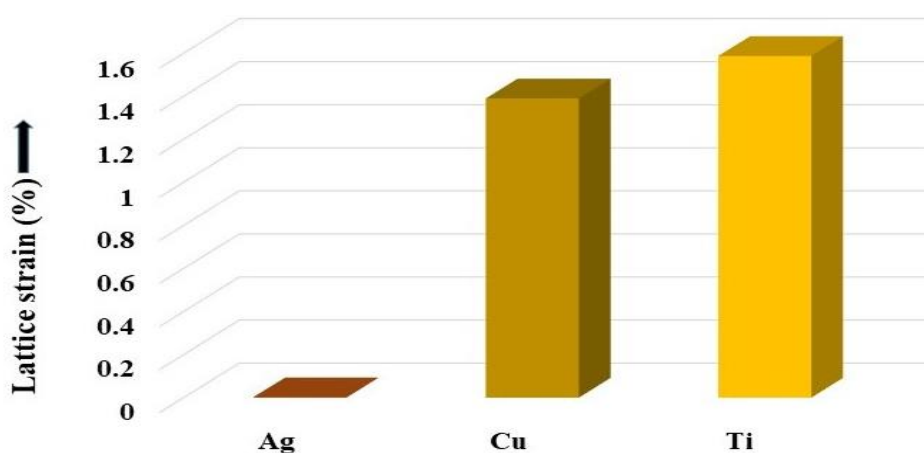


Fig. 3. Lattice strain bar chart of Ag, Cu and Ti crystals

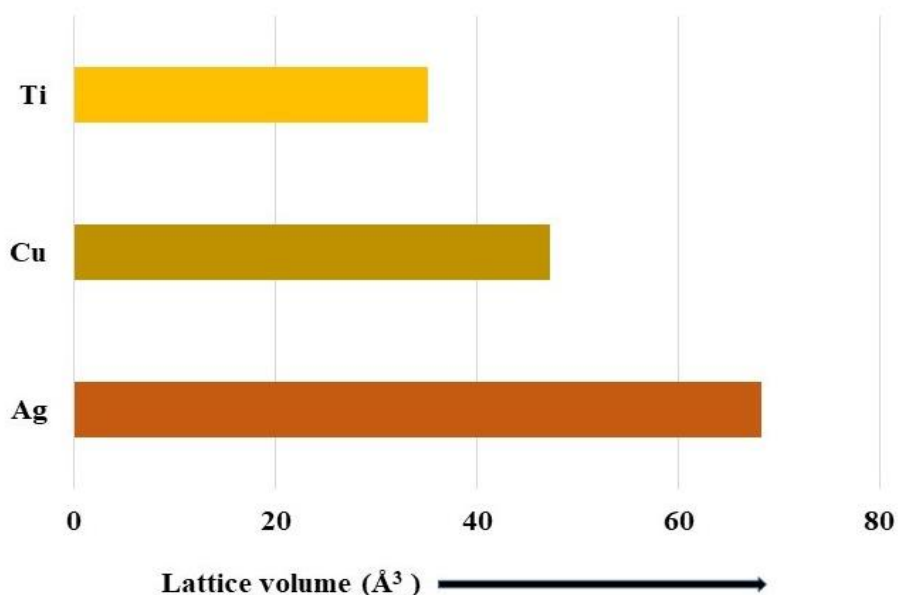


Fig. 4. Lattice volume bar chart of Ag, Cu and Ti crystals

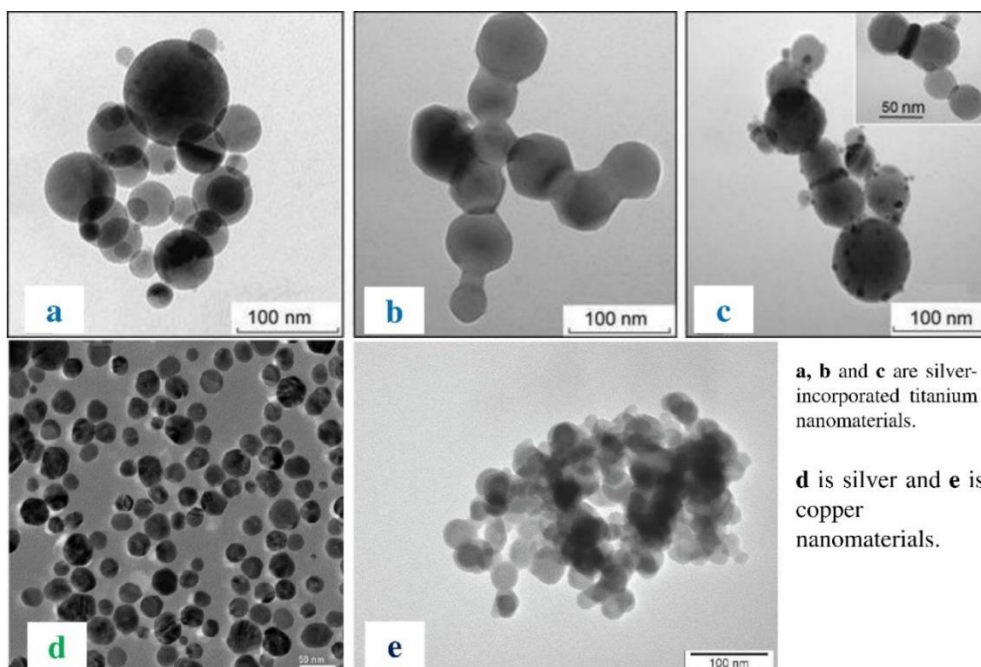


Fig. 5. Internal morphology of (a), (b), (c) for Ti [115]; (d) for Ag [113] and (e) for Cu [114] nanoparticles

The lattice volume of Ag is the largest at 68.30 Å<sup>3</sup>, followed by Cu at 47.23 Å<sup>3</sup> and Ti has the smallest lattice volume of 35.10 Å<sup>3</sup>. The difference in lattice volumes is primarily due to the different atomic radii and crystal structures of these metals. The FCC structure of Ag and Cu results in larger lattice volumes compared to the HCP structure of Ti [76].

#### 4.2 Transmission Electron Microscopic (TEM) Analysis

Fig. 5. Shows the internal morphology of the selected Ti, Ag and Cu nanoparticles. Here the Ti nanoparticles were mostly spherical with a unified distribution but no agglomeration [115] due to their electronic configuration as well as

the surface-charged emphasis on the formation of nanomaterials by a capping agent. The same result was found for Ag nanomaterials with poor agglomeration [113] by reducing agents. On the other hand, the Cu materials showed poor agglomerated and ball-shaped [114] nanoparticles with uniform distribution into the inner core-shell of the structure. The Cu nanomaterials were shown agglomerated for their highly oxidative and conductivity [114]. This phenomenon might be explored with Ti light elements rather than Cu and Ag [113-115].

Fig. 6. Shows the diffraction plane of the nanocrystals by SAED. SAED called the electron diffraction method performed in TEM measures the lattice parameters, crystal structure and extent of crystallinity of nanoparticles from the diffraction technique in which the sample is targeted with a parallel beam of high-energy electrons [34, 128]. The crystalline predominant plane such as Miller indices observed in SAED [116-118] with specified diffraction areas like 20.0 to 50.0 cm selected by diffraction nanobeam in SAED was exposed which was revealed by XRD.

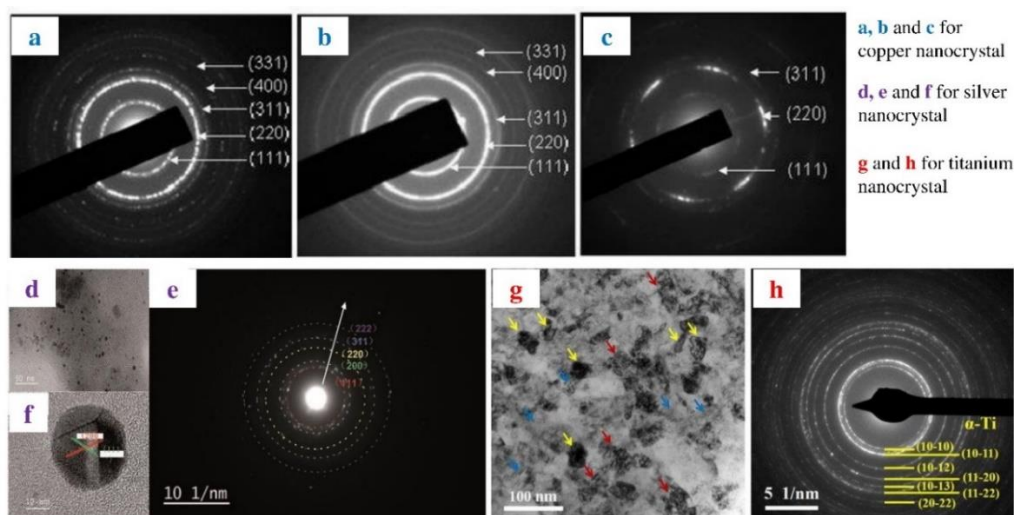


Fig. 6. Selected area electron diffraction pattern of Ag [116], Cu [117] and Ti [118] nanocrystals

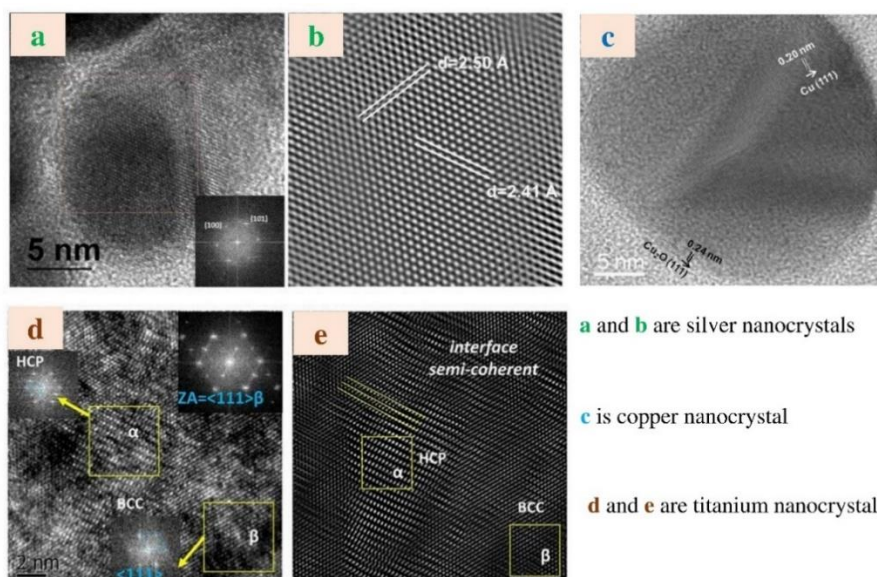


Fig. 7. HR-TEM of Ag [119], Cu [120] and Ti [121] nanocrystals

Fig. 7. depicts the high-resolution TEM which showed the interplanar distance of the nanocrystals like Ag [119], Cu [120] and Ti [121]. The planes where the atoms were uniformly distributed and arranged an alignment of the atoms of Ag [119], Cu [120] and Ti [121]. HRTEM provides direct images of the atomic structure of the particles. It explored direct information about the crystallographic texture, structure and shape of materials from images and high-phase contrast images like tiny a crystal cell could be captured [6,34,47,121].

## 5. COMPARATIVE OVERVIEW of Ag, Cu AND Ti NANOCRYSTALS FUNCTIONAL APPLICATIONS

### 5.1 Electrical Conductivity

Among all metals, Ag nanocrystals have the highest electrical conductivity. This property is attributed to the high mobility of electrons within the silver lattice which effectively transmits an electric current [106]. As a result, Ag nanoparticles are common components of electronics, circuit parts and high-performance conductive inks [77]. The second-best electrical conductor after Ag is Cu nanocrystals [107]. This metal resembles Ag, as it has a high capability for the mobility of electrons [107]. Therefore, Cu nanoparticles are used for electrical wires, power lines and electrical motor manufacturing because of use for their low cost and satisfactory conductivity [78]. Ti nanocrystals are not characterized by exceptional electrical conductivity. Despite the metal nature of Ti, it is a poor conductor in comparison to copper and Ag [94]. Therefore, Ti nanocrystals are not widely used as conductive materials [79,113]. Nonetheless, Ti is used in industries where electrical conductivity is not a priority and other qualities such as corrosion inhibition and biocompatibility are preferred. These industries include aerospace and medical implant manufacturing [70,79].

### 5.2 Corrosion Resistance

The ability of Ag nanocrystals to withstand corrosion is not well recognized. Although Ag doesn't corrode in most situations, Ag nanoparticles can undergo oxidation or other chemical reactions in specific situations [108]. To improve their durability and lessen the impacts of corrosion, Ag nanoparticles are frequently coated all over the world [80]. On the other hand, Cu nanocrystals are more likely to corrode,

particularly in humid or acidic environments. Over time, copper oxidizes and develops a green patina, or Cu oxide, on its surface [109]. However, Cu nanocrystals can be made more corrosion-resistant by surface treatments or alloying with other elements which makes them useful for a variety of applications like electrical wire, roofing and plumbing [81]. The remarkable resistance to corrosion of Ti nanocrystals is well known, especially in abrasive conditions like seawater and chemical processing. On its surface, Ti creates a protective oxide layer called titanium dioxide that stops more oxidation and corrosion [93]. Because of their intrinsic corrosion resistance, Ti nanocrystals are widely sought after in applications such as biomedical implants, chemical processing equipment and marine structures where exposure to corrosive chemicals is a concern [82-83].

### 5.3 Catalytic Activity

Ag nanocrystals are renowned for their exceptional catalytic activity, particularly in oxidation reactions of organic compounds and alcohols [110]. Their high selectivity often leads to the formation of specific products, making them valuable in catalytic converters, environmental remediation and chemical synthesis processes [84]. Cu nanocrystals, on the other hand, demonstrate versatile catalytic capabilities, participating in a wide range of reactions such as hydrogenation, dehydrogenation and C-C coupling reactions [85]. Their excellent catalytic activity stems from their ability to engage in redox reactions and they find applications in catalytic converters, carbon capture, fuel cells and organic synthesis [111,114,115]. While less common as catalysts compared to Ag and Cu, Ti nanocrystals also exhibit catalytic activity in certain reactions, including hydrogenation, photocatalysis and oxidation reactions [86]. Their selectivity can be influenced by factors such as surface morphology, crystal phase and doping with other elements. Ti nanocrystals are utilized in niche applications such as photocatalytic water splitting, environmental remediation and the synthesis of fine chemicals [87,118].

### 5.4 Antimicrobial Property

Ag, Cu and Ti nanocrystals possess distinctive antimicrobial properties, making them valuable in various applications ranging from healthcare to environmental remediation [112]. Ag nanocrystals are renowned for their potent

antimicrobial activity, attributed to the release of Ag ions ( $\text{Ag}^+$ ) that interfere with bacterial cell wall membranes and DNA, inhibiting microbial growth [88,116,119]. This characteristic has resulted in the extensive utilization of Ag nanoparticles in medical equipment, wound dressings and antimicrobial coatings applied to surfaces [89]. Similarly, Cu nanocrystals exhibit strong antimicrobial efficacy due to the release of Cu ions ( $\text{Cu}^{2+}$ ) that disrupt microbial cell membranes and proteins, leading to cell death [90, 117, 120]. Cu nanoparticles find applications in healthcare settings where they are used in hospital surfaces, door handles and medical equipment to reduce the risk of healthcare-associated infections [91]. Ti nanocrystals, although less studied for their antimicrobial properties compared to Ag and Cu, also demonstrate antimicrobial activity through mechanisms such as photocatalysis and surface modification [92, 121] as well as any materials that have unique functional applications [122-132] in different approaches.

## 6. CONCLUSION

This manuscript has presented a thorough crystallographic comparison of functional nanocrystals of Ag, Cu and Ti using both TEM and XRD techniques. By systematically analyzing data from a large number of studies, significant insights have been gained into the formation mechanisms and structural characteristics of these important nanomaterials. It has highlighted the key similarities and differences in the crystallographic biography of the three nanocrystal systems. While all three metals Ag, Cu and Ti can form a variety of crystalline phases and morphologies, subtle variations in synthetic parameters profoundly impact the resulting nanostructures. These crystallographic details, in turn, dictate the functional properties relevant to applications. The degree of crystallinity in nanocrystalline materials was observed at 90.0%, 98.0% and 100.0% of Ti, Cu and Ag respectively. This quantitative comparison provides valuable insights into the structural property relationships in these nanocrystals, enabling rational design strategies for optimizing their performance in various functional applications. Furthermore, these crystalline nanomaterials might be used as an antimicrobial agent for ceramic coating or substrate for its functional approaches.

## ACKNOWLEDGEMENTS

The authors expressed their heartfelt thanks to Dr. Shirin Akter Jahan, PSO, BCSIR and Dr. Samina Ahmed, CSO & Director, IGCRT, BCSIR for their cooperation and use of the software and PC. We also expressed thanks to Dr. Sharif Md. Al-Reza, Professor & Chairman, Department of Applied Chemistry and Chemical Engineering (ACCE), Islamic University, Kushtia-7003, Bangladesh for the kind cooperation and access to the laboratory facilities and software.

## COMPETING INTERESTS

The authors have declared that there is no competing or financial interests exist.

## REFERENCES

1. Kumar R. Analysis and visualisation of research trends in nanomaterial: A general review. *Turkish Journal of Computer and Mathematics Education (TURCOMAT)*. 2021;12(2):2959-2964.
2. Baig N, Kammakam I, Falath W. Nanomaterials: A review of synthesis methods, properties, recent progress, and challenges. *Materials Advances*. 2021; 2(6):1821-1871.
3. Kang J, Li F, Xu Z, Chen X, Sun M, Li Y, Guo L. How Amorphous Nanomaterials Enhanced Electrocatalytic, SERS, and Mechanical Properties. *JACS Au*. 2023; 3(10):2660-2676.
4. Ramli NH, Nor NM, Hakimi A, Zakaria ND, Lockman Z, Razak KA. Platinum-based nanoparticles: A review of synthesis methods, surface functionalization, and their applications. *Microchemical Journal*. 2024;110280.
5. Ghosh S, Sagayam KM, Haldar D, Jone AAA, Acharya B, Gerogiannis VC, Kanavos A. A review on the types of nanomaterials and methodologies used for the development of biosensors. *Advances in Natural Sciences: Nanoscience and Nanotechnology*. 2024;15(1):013001.
6. Alam MA, Bishwas RK, Mostofa S, Jahan SA. Crystallographic phase stability of nanocrystalline polymorphs  $\text{TiO}_2$  by tailoring hydrolysis pH. *South African Journal of Chemical Engineering*; 2024.
7. Bykkam S, Ahmadipour M, Narisngam S, Kalagadda VR, Chidurala SC. Extensive studies on X-ray diffraction of green

- synthesized silver nanoparticles. *Adv. Nanopart.* 2015;4(1):1-10.
8. Alshareef A. An investigation into the effects of shape and structure on the antibacterial efficacy of metal nanoparticles (Doctoral dissertation, De Montfort University); 2019.
  9. Kobir MM, Tabassum S, Ahmed S, Sadia SI, Alam MA. Crystallographic benchmarking on diffraction pattern profiling of Polymorphs-TiO<sub>2</sub> by WPPF for Pigment and Acrylic Paint. *Archives of Current Research International.* 2024; 24(1):62-70.
  10. Agrawal S, Bhatt M, Rai SK, Bhatt A, Dangwal P, Agrawal PK. Silver nanoparticles and its potential applications: A review. *Journal of Pharmacognosy and Phytochemistry.* 2018;7(2):930-937.
  11. Ghanghas P, Jangid NK, Poonia K. Advanced composites of nanomaterials and their applications. in advanced composites. Cham: Springer Nature Switzerland. 2023;37-58.
  12. Kang DK, Moon SK, Oh KT, Choi GS, Kim KN. Properties of experimental titanium-silver-copper alloys for dental applications. *Journal of Biomedical Materials Research Part B: Applied Biomaterials.* 2009;90(1):446-451.
  13. Alavi M, Karimi N. Characterization, antibacterial, total antioxidant, scavenging, reducing power and ion chelating activities of green synthesized silver, copper and titanium dioxide nanoparticles using *Artemisia haussknechtii* leaf extract. *Artificial cells, Nanomedicine, and Biotechnology.* 2018;4(6):8, 2066-2081.
  14. Wysocka I, Kowalska E, Ryl J, Nowaczyk G, Zielińska-Jurek A. Morphology, photocatalytic and antimicrobial properties of TiO<sub>2</sub> modified with mono-and bimetallic copper, platinum and silver nanoparticles. *Nanomaterials.* 2019;9(8):1129.
  15. Dikshit PK, Kumar J, Das AK, Sadhu S, Sharma S, Singh S, Kim BS. Green synthesis of metallic nanoparticles: Applications and limitations. *Catalysts.* 2021;11(8):902.
  16. Charitidis CA, Georgiou P, Koklioti MA, Trompeta AF, Markakis V. Manufacturing nanomaterials: from research to industry. *Manufacturing Review.* 2014;1:11.
  17. Kiran JU, Roners JP, Mathew S. XPS and thermal studies of silver doped SiO<sub>2</sub> matrices for plasmonic applications. *Materials Today: Proceedings.* 2020;33: 1263-1267.
  18. Ahmed F, Kanoun MB, Awada C, Jonin C, Brevet PF. An experimental and theoretical study on the effect of silver nanoparticle concentration on the structural, morphological, optical, and electronic properties of TiO<sub>2</sub> nanocrystals. *Crystals.* 2021;11(12):1488.
  19. García DA, Mendoza L, Vizuete K, Debut A, Arias MT, Gavilanes A, Dahoumane SA. Sugar-mediated green synthesis of silver selenide semiconductor nanocrystals under ultrasound irradiation. *Molecules.* 2020;25(21):5193.
  20. Torres-Flores EI, Flores-López NS, Martínez-Núñez CE, Tánori-Córdova JC, Flores-Acosta M, Cortez-Valadez M. Silver nanoparticles in natural zeolites incorporated into commercial coating: antibacterial study. *Applied Physics A.* 2021;127:1-11.
  21. Yu W, Xie H, Chen L, Li Y, Zhang C. Synthesis and characterization of monodispersed copper colloids in polar solvents. *Nanoscale Research Letters.* 2009;4:465-470.
  22. LaGrow AP, Sinatra L, Elshewy A, Huang KW, Katsiev K, Kirmani AR, Bakr OM. Synthesis of copper hydroxide branched nanocages and their transformation to copper oxide. *The Journal of Physical Chemistry C.* 2014;118(33):19374-19379.
  23. Dharmadasa R, Jha M, Amos DA, Druffel T. Room temperature synthesis of a copper ink for the intense pulsed light sintering of conductive copper films. *ACS Applied Materials and Interfaces.* 2013; 5(24):13227-13234.
  24. Zhu HT, Zhang CY, Yin YS. Rapid synthesis of copper nanoparticles by sodium hypophosphite reduction in ethylene glycol under microwave irradiation. *Journal of Crystal Growth.* 2004;270(3-4):722-728.
  25. Moghimi-Rad J, Zabihi F, Hadi I, Ebrahimi S, Isfahani TD, Sabbaghzadeh J. Effect of ultrasound radiation on the size and size distribution of synthesized copper particles. *Journal of Materials Science.* 2010;45(14): 3804-3811.
  26. Wang YN, Duan X, Zheng J, Lin H, Yuan Y, Ariga H, Asakura K. Remarkable enhancement of Cu catalyst activity in hydrogenation of dimethyl oxalate to ethylene glycol using gold. *Catalysis*

- Science and Technology. 2012;2(8):1637-1639.
27. Sugimoto T, Zhou X, Muramatsu A. Synthesis of uniform anatase TiO<sub>2</sub> nanoparticles by gel-sol method: 3. Formation process and size control. *Journal of Colloid and Interface Science*. 2003;259(1):43-52.
  28. Tripathi AK, Mathpal MC, Kumar P, Singh MK, Mishra SK, Srivastava RK, Agarwal A. Synthesis-based structural and optical behavior of anatase TiO<sub>2</sub> nanoparticles. *Materials Science in Semiconductor Processing*. 2014;23:136-143.
  29. Thapa R, Maiti S, Rana TH, Maiti UN, Chattopadhyay KK. Anatase TiO<sub>2</sub> nanoparticles synthesis via simple hydrothermal route: Degradation of Orange II, Methyl Orange and Rhodamine B. *Journal of Molecular Catalysis A: Chemical*. 2012;363:223-229.
  30. Kong W, Chen C, Mai K, Shi X, Hu R, Wang Z. Large-scale synthesis and self-assembly of monodisperse spherical TiO<sub>2</sub>nanocrystals. *Journal of Nanomaterials*. 2011;1-4.
  31. Mazhar F, Kausar A, Iqbal M. Photocatalytic hydrogen generation using TiO<sub>2</sub>: A state-of-the-art review. *Zeitschrift für Physikalische Chemie*. 2022;236(11-12):1697-1728.
  32. Ahamed MS, Ali MS, Ahmed S, Sadia SI, Islam MR, Rahaman MA, Alam MA. Synthesis of Silver Nanomaterials Capping by Fruit-mediated Extracts and Antimicrobial Activity: A Critical Review. *International Research Journal of Pure and Applied Chemistry*. 2024;25(1):45-60.
  33. Tabassum M, Alam MA, Mostofa S, Bishwas RK, Sarkar D, Jahan SA. Synthesis and crystallinity integration of copper nanoparticles by reaction medium. *Journal of Crystal Growth*. 2024;626:127486.
  34. Alam MA, Bishwas RK, Mostofa S, Jahan SA. Low-temperature synthesis and crystal growth behaviour of nanocrystal anatase-TiO<sub>2</sub>. *Materials Letters*. 2024;354:135396.
  35. Alam MA, Tabassum M, Mostofa S, Bishwas RK, Sarkar D, Jahan SA. The effect of precursor concentration on the crystallinity synchronization of synthesized copper nanoparticles. *Journal of Crystal Growth*. 2023;621:127386.
  36. Alam MA, Mobashsara MT, Sabrina SM, Bishwas RKB, Debasish DS, Shirin SAJ. One-pot low-temperature synthesis of high crystalline cu nanoparticles. *Malaysian Journal of Science and Advanced Technology*. 2023;122-127.
  37. Alam MA, Munni SA, Mostafa S, Bishwas RK, Jahan SA. An investigation on a synthesis of silver nanoparticles. *Asian Journal of Research in Biochemistry*. 2023;12(3):1-10.
  38. Giannini C, Ladisa M, Altamura D, Siliqi D, Sibillano T, De Caro L. X-ray diffraction: A powerful technique for the multiple-length-scale structural analysis of nanomaterials. *Crystals*. 2016;6(8):87.
  39. Bushell M, Beauchemin S, Kunc F, Gardner D, Ovens J, Toll F, Johnston LJ. Characterization of commercial metal oxide nanomaterials: Crystalline phase, particle size and specific surface area. *Nanomaterials*. 2020;10(9):1812.
  40. Gharibshahi L, Saion E, Gharibshahi E, Shaari AH, Matori KA. Structural and optical properties of Ag nanoparticles synthesized by thermal treatment method. *Materials*. 2017;10(4):402.
  41. Mahdiah M, Zolanvari A, Azimee AS. Green biosynthesis of silver nanoparticles by *Spirulina platensis*. *Scientia Iranica*. 2012;19(3):926-929.
  42. Pathak TK, Kroon RE, Swart HC. Photocatalytic and biological applications of Ag and Au doped ZnO nanomaterial synthesized by combustion. *Vacuum*. 2018;157:508-513.
  43. Babu MG, Gunasekaran P. Production and structural characterization of crystalline silver nanoparticles from *Bacillus cereus* isolate. *Colloids and surfaces B: Biointerfaces*. 2009;74(1):191-195.
  44. Forough M, Farhadi K. Biological and green synthesis of silver nanoparticles. *Turkish J. Eng. Env. Sci*. 2010;34(4):281-287.
  45. Shamel K, Bin Ahmad M, Jaffar Al-Mulla EA, Ibrahim NA, Shabanzadeh P, Rustaiyan A, Zidan M. Green biosynthesis of silver nanoparticles using *Callicarpa maingayi* stem bark extraction. *Molecules*. 2012;17(7):8506-8517.
  46. Al-thabaiti SA, Obaid AY, Khan Z, Bashir O, Hussain S. Cu nanoparticles: Synthesis, crystallographic characterization, and stability. *Colloid and Polymer Science*. 2015;293:2543-2554.
  47. Tabassum M, Alam MA, Mostofa S, Bishwas RK, Sarkar D, Jahan SA. Synthesis and crystallinity integration of copper nanoparticles by reaction medium.

- Journal of Crystal Growth. 2024;626:127486.
48. Alam MA, Mobashsara MT, Sabrina SM, Bishwas RKB, Debasish DS, Shirin SAJ. One-pot low-temperature synthesis of high crystalline Cu nanoparticles. Malaysian Journal of Science and Advanced Technology. 2023;122-127.
  49. Khan A, Rashid A, Younas R, Chong R. A chemical reduction approach to the synthesis of copper nanoparticles. International Nano Letters. 2016;6:21-26.
  50. Li H, Cai W. Understanding the deformation mechanism of individual phases of a dual-phase beta type titanium alloy using in situ diffraction method. Materials Science and Engineering: A. 2018;728:151-156.
  51. Yan M, Luo SD, Schaffer GB, Qian M. TEM and XRD characterisation of commercially pure  $\alpha$ -Ti made by powder metallurgy and casting. Materials Letters. 2012;72:64-67.
  52. Gemelli E, Camargo NHA. Oxidation kinetics of commercially pure titanium. Matéria (Rio de Janeiro). 2007;12:525-531.
  53. Bieler TR, Wang L, Beaudoin AJ, Kenesei P, Lienert U. In situ characterization of twin nucleation in pure Ti using 3D-XRD. Metallurgical and Materials Transactions A. 2014;45:109-122.
  54. Kolli RP, Devaraj A. A review of metastable beta titanium alloys. Metals. 2018;8(7):506.
  55. Ghosh A, Singh A, Gurao NP. Effect of rolling mode and annealing temperature on microstructure and texture of commercially pure-titanium. Materials Characterization. 2017;125:83-93.
  56. Mabrouk MM, Mansour AT, Abdelhamid AF, Abualnaja KM, Mamoon A, Gado WS, Ayoub HF. Impact of aqueous exposure to silver nanoparticles on growth performance, redox status, non-specific immunity, and histopathological changes of Nile Tilapia, *Oreochromis niloticus*, challenged with *Aeromonas hydrophila*. Aquaculture Reports. 2021;21:100816.
  57. Phul R, Kaur C, Farooq U, Ahmad T. Ascorbic acid assisted synthesis, characterization and catalytic application of copper nanoparticles. Mater. Sci. Eng. Int. J. 2018;2(4):90-94.
  58. Balbinotti P, Gemelli E, Buerger G, Lima SAD, Jesus JD, Camargo NHA, Soares GDDA. Microstructure development on sintered Ti/HA biocomposites produced by powder metallurgy. Materials Research. 2011;14:384-393.
  59. Zhong J, Zhang LH, Jin ZH, Sui ML, Lu K. Superheating of Ag nanoparticles embedded in Ni matrix. Acta materialia. 2001;49(15):2897-2904.
  60. Sastry ABS, Karthik Aamanchi RB, Sree Rama Linga Prasad C, Murty BS. Large-scale green synthesis of Cu nanoparticles. Environmental Chemistry Letters. 2013;11:183-187.
  61. Abe Y, Matsui E, Senna M. Preparation of phase pure and well-crystallized  $\text{Li}_4\text{Ti}_5\text{O}_{12}$  nanoparticles by precision control of starting mixture and calcining at lowest possible temperatures. Journal of Physics and Chemistry of Solids. 2007;68(5-6):681-686.
  62. Pang YX, Bao X. Influence of temperature, ripening time and calcination on the morphology and crystallinity of hydroxyapatite nanoparticles. Journal of the European Ceramic Society. 2003;23(10):1697-1704.
  63. Jain A, Ong SP, Hautier G, Chen W, Richards WD, Dacek S, Persson KA. Commentary: The Materials Project: A materials genome approach to accelerating materials innovation. APL Materials. 2013;1(1).
  64. Kamb WB. Theory of preferred crystal orientation developed by crystallization under stress. The Journal of Geology. 1959;67(2):153-170.
  65. Pan H, Sun H, Poh C, Feng Y, Lin J. Single-crystal growth of metallic nanowires with preferred orientation. Nanotechnology. 2005;16(9):1559.
  66. Wang Y, Ghanbaja J, Soldera F, Boulet P, Horwat D, Mücklich F, Pierson JF. Controlling the preferred orientation in sputter-deposited  $\text{Cu}_2\text{O}$  thin films: Influence of the initial growth stage and homoepitaxial growth mechanism. Acta Materialia. 2014;76:207-212.
  67. Keeler JH, Geisler AH. Preferred orientations in rolled and annealed titanium. JOM. 1956;8(2):80-90.
  68. Miao Y, Zhao Y, Zhang S, Shi R, Zhang T. Strain engineering: A boosting strategy for photocatalysis. Advanced Materials. 2022;34(29):2200868.
  69. Sun Y, Ren Y, Liu Y, Wen J, Okasinski JS, Miller DJ. Ambient-stable tetragonal phase in silver nanostructures. Nature Communications. 2012;3(1):971.

70. Zheng Y, Li X, Cheng X, Li Z, Liu Y, Dong C. Enhanced thermal stability of Cu alloy films by strong interaction between Ni and Zr (or Fe). *Journal of Physics D: Applied Physics*. 2018;51(13):135304.
71. Alloys ZSMHS. *First-principles Studies on the Structures and Properties of Ti-and*; 2013.
72. Tilley RJ. *Crystals and crystal structures*. John Wiley and Sons; 2020.
73. Yamamura A, Maruoka S, Ohtsuka J, Miyakawa T, Nagata K, Kataoka M, Tanokura M. Expression, purification, crystallization and preliminary X-ray analysis of conjugated polyketone reductase C2 (CPR-C2) from *Candida parapsilosis* IFO 0708. *Acta Crystallographica Section F: Structural Biology and Crystallization Communications*. 2009;65(11):1145-1148.
74. Hebbaz A, Belhani M, Tahraoui T. Synthesis of cerium-doped magnesium spinel ferrites and study of their physical properties for photocatalytic applications under sunlight irradiation. *Applied Physics A*. 2024;130(2):1-14.
75. Gupta R, Kim EY, Shin HS, Lee GY, Yeo DH. Structural, microstructural, and microwave dielectric properties of (Al<sub>1-x</sub>B<sub>x</sub>)<sub>2</sub>Mo<sub>3</sub>O<sub>12</sub> ceramics with low dielectric constant and low dielectric loss for LTCC applications. *Ceramics International*. 2023;49(14):22690-22701.
76. Manna I, Chattopadhyay PP, Nandi P, Banhart F, Fecht HJ. Formation of face-centered-cubic titanium by mechanical attrition. *Journal of Applied Physics*. 2003;93(3):1520-1524.
77. Mahendia S, Tomar AK, Kumar S. Electrical conductivity and dielectric spectroscopic studies of PVA–Ag nanocomposite films. *Journal of Alloys and Compounds*. 2010;508(2):406-411.
78. Sivasubramaniam V, Ramasamy S, Venkatraman M, Gatto G, Kumar A. Carbon nanotubes as an alternative to copper wires in electrical machines: A review. *Energies*. 2023;16(9):3665.
79. Kaur M, Singh K. Review on titanium and titanium based alloys as biomaterials for orthopaedic applications. *Materials Science and Engineering: C*. 2019;102:844-862.
80. Asaad MA, Ismail M, Tahir MM, Huseien GF, Raja PB, Asmara YP. Enhanced corrosion resistance of reinforced concrete: Role of emerging eco-friendly *Elaeis guineensis*/silver nanoparticles inhibitor. *Construction and Building Materials*. 2018;188:555-568.
81. Bastidas DM, Criado M, Fajardo S, La Iglesia VM, Cano E, Bastidas JM. Copper deterioration: Causes, diagnosis and risk minimisation. *International Materials Reviews*. 2010;55(2):99-127.
82. Al Othman ZA, Alam MM, Naushad M, Inamuddin I, Khan MF. Inorganic nanoparticles and nanomaterials based on titanium (Ti): applications in medicine. In *Materials Science Forum*. Trans Tech Publications Ltd. 2013;754:21-87.
83. Zhang LC, Chen LY, Wang L. Surface modification of titanium and titanium alloys: Technologies, developments, and future interests. *Advanced Engineering Materials*. 2020;22(5):1901258.
84. Dong XY, Gao ZW, Yang KF, Zhang WQ, Xu LW. Nanosilver as a new generation of silver catalysts in organic transformations for efficient synthesis of fine chemicals. *Catalysis Science and Technology*. 2015;5(5):2554-2574.
85. Gawande MB, Goswami A, Felpin FX, Asefa T, Huang X, Silva R, Varma RS. Cu and Cu-based nanoparticles: Synthesis and applications in catalysis. *Chemical Reviews*. 2016;116(6):3722-3811.
86. Jeon JP, Kweon DH, Jang BJ, Ju MJ, Baek JB. Enhancing the photocatalytic activity of TiO<sub>2</sub> catalysts. *Advanced Sustainable Systems*. 2020;4(12):2000197.
87. Ma Y, Wang X, Jia Y, Chen X, Han H, Li C. Titanium dioxide-based nanomaterials for photocatalytic fuel generations. *Chemical Reviews*. 2014;114(19):9987-10043.
88. Le Ouay B, Stellacci F. Antibacterial activity of silver nanoparticles: A surface science insight. *Nano Today*. 2015;10(3):339-354.
89. Knetsch ML, Koole LH. New strategies in the development of antimicrobial coatings: The example of increasing usage of silver and silver nanoparticles. *Polymers*. 2011;3(1):340-366.
90. Milojkov, D. V., Radosavljević-Mihajlović, A. S., Stanić, V. D., Nastasijević, B. J., Radotić, K., Janković-Častvan I, Živković-Radovanović V. Synthesis and characterization of luminescent Cu<sup>2+</sup>-doped fluorapatite nanocrystals as potential broad-spectrum antimicrobial

- agents. *Journal of Photochemistry and Photobiology B: Biology*. 2023;239:112649.
91. Bisht N, Dwivedi N, Kumar P, Venkatesh M, Yadav AK, Mishra D, Dhand C. Recent advances in copper and copper-derived materials for antimicrobial resistance and infection control. *Current Opinion in Biomedical Engineering*. 2022;24:100408.
  92. Chouirfa H, Bouloussa H, Migonney VU, Falentin-Daudré C. Review of titanium surface modification techniques and coatings for antibacterial applications. *Acta Biomaterialia*. 2019;83:37-54.
  93. Das R, Ambardekar V, Bandyopadhyay PP. Titanium dioxide and its applications in mechanical, electrical, optical, and biomedical fields (Vol. 7). London, UK: In tech Open; 2021.
  94. Gulbiński W, Suszko T, Sienicki W, Warcholiński B. Tribological properties of silver-and copper-doped transition metal oxide coatings. *Wear*. 2003;254(1-2):129-135.
  95. Cheng YQ, Ma E. Atomic-level structure and structure–property relationship in metallic glasses. *Progress in Materials Science*. 2011;56(4):379-473.
  96. Wenk HR. (Ed.). Preferred orientation in deformed metal and rocks: An introduction to modern texture analysis. Elsevier; 2013.
  97. Lütjering G, Williams JC, Gysler A. Microstructure and mechanical properties of titanium alloys. In *Microstructure and Properties of Materials*. 2000;2:1-77.
  98. Withers PJ, Preuss M, Steuwer A, Pang J. Methods for obtaining the strain-free lattice parameter when using diffraction to determine residual stress. *Journal of Applied Crystallography*. 2007;40(5):891-904.
  99. Smallman RE, Bishop RJ. Metals and materials: Science, processes, applications. Elsevier; 2013.
  100. Warwick JLW, Jones NG, Rahman KM, Dye D. Lattice strain evolution during tensile and compressive loading of CP Ti. *Acta Materialia*. 2012;60(19):6720-6731.
  101. Nan XL, Wang HY, Wu ZQ, Xue ES, Zhang L, Jiang QC. Effect of c/a axial ratio on Schmid factors in hexagonal close-packed metals. *Scripta Materialia*. 2013; 68(7):530-533.
  102. Zhang JP, Liao PQ, Zhou HL, Lin RB, Chen XM. Single-crystal X-ray diffraction studies on structural transformations of porous coordination polymers. *Chemical Society Reviews*. 2014;43(16):5789-5814.
  103. Şelte A, Özkal B. Crystallite size and strain calculations of hard particle reinforced composite powders (Cu/Ni/Fe–WC) synthesized via mechanical alloying. *Proceedings of the Estonian Academy of Sciences*. 2019;68(1):66-78.
  104. Mara NA, Beyerlein IJ. Effect of bimetal interface structure on the mechanical behavior of Cu–Nb fcc–bcc nanolayered composites. *Journal of Materials Science*. 2014;49:6497-6516.
  105. Ali MH, Azad MAK, Khan KA, Rahman MO, Chakma U, Kumer A. Analysis of crystallographic structures and properties of silver nanoparticles synthesized using PKL extract and nanoscale characterization techniques. *ACS Omega*. 2023;8(31):28133-28142.
  106. Khalil AM, Hassan ML, Ward AA. Novel nanofibrillated cellulose/polyvinylpyrrolidone/silver nanoparticles films with electrical conductivity properties. *Carbohydrate Polymers*. 2017;157:503-511.
  107. Hernandez-Castaneda JC, Lok BK, Zheng H. Laser sintering of Cu nanoparticles on PET polymer substrate for printed electronics at different wavelengths and process conditions. *Frontiers of Mechanical Engineering*. 2020;15:303-318.
  108. Levard C, Hotze EM, Lowry GV, Brown Jr GE. Environmental transformations of silver nanoparticles: Impact on stability and toxicity. *Environmental Science and Technology*. 2012;46(13):6900-6914.
  109. Leygraf C, Chang T, Herting G, Wallinder IO. The origin and evolution of copper patina colour. *Corrosion Science*. 2019; 157:337-346.
  110. Dong XY, Gao ZW, Yang KF, Zhang WQ, Xu LW. Nanosilver as a new generation of silver catalysts in organic transformations for efficient synthesis of fine chemicals. *Catalysis Science and Technology*. 2015; 5(5):2554-2574.
  111. Dey S, Dhal GC. Controlling carbon monoxide emissions from automobile vehicle exhaust using copper oxide catalysts in a catalytic converter. *Materials Today Chemistry*. 2020;17:100282.
  112. Makvandi P, Wang CY, Zare EN, Borzacchiello A, Niu LN, Tay FR. Metal-based nanomaterials in biomedical applications: Antimicrobial activity and

- cytotoxicity aspects. *Advanced Functional Materials*. 2020;30(22):1910021.
113. Chou KS, Huang KC, Lee HH. Fabrication and sintering effect on the morphologies and conductivity of nano-Ag particle films by the spin coating method. *Nanotechnology*. 2005;16(6):779.
114. Mroczek-Sosnowska N, Sawosz E, Vadalasetty KP, Łukasiewicz M, Niemiec J, Wierzbicki M, Chwalibog A. Nanoparticles of copper stimulate angiogenesis at systemic and molecular level. *International Journal of Molecular Sciences*. 2015;16(3):4838-4849.
115. Svarovskaya NV, Bakina OV, Pervikov AV, Rubtsov KV, Lerner MI. Electrical explosion of wires for manufacturing bimetallic antibacterial Ti–Ag and Fe–Ag Nanoparticles. *Russian Physics Journal*. 2020;62:1580-1586.
116. Cai Y, Piao X, Gao W, Zhang Z, Nie E, Sun Z. Large-scale and facile synthesis of silver nanoparticles via a microwave method for a conductive pen. *RSC Advances*. 2017;7(54):34041-34048.
117. Shen H, Wang H, Yuan H, Ma L, Li LS. Size-, shape-, and assembly-controlled synthesis of Cu<sub>2-x</sub>Se nanocrystals via a non-injection phosphine-free colloidal method. *CrystEngComm*. 2012;14(2):555-560.
118. Zhang B, Wang J, Zhu S, Zhu N, Zhang J, Wang Z. Effects of ECAP on the formation and tribological properties of thermal oxidation layers on a pure titanium surface. *Oxidation of Metals*. 2019;91:483-494.
119. Virgen-Ortiz A, Limón-Miranda S, Soto-Covarrubias MA, Apolinar-Iribe A, Rodríguez-León E, Iñiguez-Palomares R. Biocompatible silver nanoparticles synthesized using rumex hymenosepalus extract decreases fasting glucose levels in diabetic rats. *Dig. J. Nanomater. Biostruct*. 2015;10(3):927-933.
120. Cheng G, Hight Walker AR. Transmission electron microscopy characterization of colloidal copper nanoparticles and their chemical reactivity. *Analytical and Bioanalytical Chemistry*. 2010;396:1057-1069.
121. Kou W, Sun Q, Xiao L, Sun J. Superior plasticity stability and excellent strength in Ti-55531 alloy micropillars via harmony slip in nanoscale  $\alpha/\beta$  phases. *Scientific Reports*. 2019;9(1):5075.
122. Haque NN, Alam MA, Roy CK, Zenat M, Akther E, Munshi JL. Cyanobacteria mediated CO<sub>2</sub> segregation: A promising alternative method for sustainable bioremediation and biomass production. *Asian Journal of Research in Biochemistry*. 2023;13(3):28-43.
123. Islam MR, Ahmed S, Sadia SI, Sarkar AK, Alam MA. Comprehensive review of phytochemical content and applications from *Cestrum nocturnum*: A Comparative Analysis of Physicochemical Aspects. *Asian Journal of Research in Biochemistry*. 2023;13(4):43-58.
124. Sarkar AK, Ahmed S, Sadia SI, Kobir MM, Tabassum S, Islam MR, Alam MA. Overview of the skeleton significance of toothpaste formulation, evaluation and historical perspectives: Insights from Bangladesh's toothpaste industry. *Journal of Materials Science Research and Reviews*. 2024;7(1):80-101.
125. Khatun M, Kobir MM, Miah MAR, Sarkar AK, Alam MA. Technologies for remediation of heavy metals in environment and ecosystem: A critical overview of comparison study. *Asian Journal of Environment and Ecology*. 2024;23(4):61-80.
126. Zenat M, Akther E, Haque NN, Hasan MR, Begum M, Munshi JL, Alam MA. Antifungal Activity of Various Plant Extracts against *Aspergillus* and *Penicillium* Species Isolated from Leather-Borne Fungus. *Microbiology Research Journal International*. 2024;34(1):10-23.
127. Kobir MM, Ali MS, Ahmed S, Sadia SI, Alam MA. Assessment of the physicochemical characteristic of wastewater in Kushtia and Jhenaidah Municipal Areas Bangladesh: A Study of DO, BOD, COD, TDS and MPI. *Asian Journal of Geological Research*. 2024;7(1):21-30.
128. Bishwas RK, Mostofa S, Alam MA, Jahan SA. Removal of malachite green dye by sodium dodecyl sulfate modified bentonite clay: Kinetics, thermodynamics and isotherm modelling. *Next Nanotechnology*. 2023;3:100021.
129. Rahman MM, Maniruzzaman M, Yeasmin MS, Gafur MA, Shaikh MAA, Alam MA, Quddus MS. Adsorptive abatement of Pb<sup>2+</sup> and crystal violet using chitosan-modified coal nanocomposites: A down flow column study. *Groundwater for Sustainable Development*. 2023;23:101028.

130. Moulick SP, Hossain MS, Al Mamun MZU, Jahan F, Ahmed MF, Sathee RA, Islam F. Characterization of waste fish bones (Heteropneustes fossilis and Otolithoides pama) for photocatalytic degradation of Congo red dye. Results in Engineering. 2023;20:101418.
131. Hasan MR, Abdur R, Alam MA, Aziz S, Sujan A, Islam D, Hossain M. Exploring the effects of different parameters on the incorporation of K ions in eggshell-derived CaO reveals highly variable catalytic efficiency for biodiesel conversion. South African Journal of Chemical Engineering. 2024;47(1):67-74.
132. Haque NN, Alam MA, Baidya AS, Zenat EA, Rahman MZ, Roy CK, Munshi JL. Bioremedial capacity of indigenous hydrophytes and microalgae of Bangladesh: A comparative study on their potential in tannery effluent treatment. Asian Journal of Environment and Ecology. 2024;23(6):53–65. Available: <https://doi.org/10.9734/ajee/2024/v23i6554>

---

© Copyright (2024): Author(s). The licensee is the journal publisher. This is an Open Access article distributed under the terms of the Creative Commons Attribution License (<http://creativecommons.org/licenses/by/4.0>), which permits unrestricted use, distribution, and reproduction in any medium, provided the original work is properly cited.

*Peer-review history:*  
The peer review history for this paper can be accessed here:  
<https://www.sdiarticle5.com/review-history/116728>